Inconsistent Regolith Thermal Control of Hydrogen Distributions at the Moon's South Pole. T. P. McClanahan[1] (timothy.p.mcclanahan@nasa.gov), I. Mitrofanov[2], W. V. Boynton[3], G. Chin[1], M. Litvak[2], T. Livengood[4], A. Sanin[2], R. D. Starr[3], J. Su[4], D. Hamara[3], K. Harshman[3], [1]NASA Goddard Space Flight Center, Bldg. 34 Room W218, Greenbelt, MD 20771 USA. [2]Institute for Space Research, Moscow, Russia, [3]Lunar and Planet. Lab., Univ. Ariz., Tucson AZ USA, [3]The Catholic Univ. Wash. D.C. USA, [4]Univ. of Mary., College Park MD USA.

Introduction: For over fifty years, intense interest has focused on determining if, where, and how much hydrogen (H) may be found near the Moon's poles [1]. Driving the ongoing interest has been the critical role that H volatiles must play as a resource for human missions [2]. Now, with several lines of evidence consistently indicating that H concentrations are enhanced in some permanently shadowed regions (PSRs), plus the possibility of diurnally-dependent volatile H concentrations [3-8], investigations are shifting towards understanding the sources of H and factors that govern concentrations. For the last seven-plus years, the Lunar Reconnaissance Orbiter (LRO) has collected an unparalleled temporal and spatial record of geophysical factors that may govern the Moon's H distribution [9].

Low temperatures in the PSRs are thought to reduce the loss of H volatiles, leaving them concentrated in PSRs [1]. In this study we correlate the lunar south polar hydrogen map with maps of known thermo-physical factors, specifically the maximum surface temperature. Analysis considers co-registered south polar hydrogen maps above 83°S, LRO's Lunar Exploration Neutron Detector (LEND) is correlated to topography and illumination maps from the Lunar Observing Laser Altimeter (LOLA), also maximum temperature maps from the Diviner radiometer (DLRE) [10-13].

Background and Methods: The south polar hydrogen map in *Fig.* 1 was produced by integrating nearly seven years of observations from LEND's collimated sensor for epithermal neutrons (CSETN). CSETN's design includes a ^{10}B/polyethylene collimator to restrict detected neutrons to a 5.6° half-angle about the instrument boresight. The collimator surrounds four nadir-pointing ^{3}He detectors that integrate at a 1-Hz rate. Hydrogen values were derived from a model-dependent measure of the neutron-flux suppression as compared to the average neutron flux measured between 55°S to 60°S [14]. Units are in weight percent water-equivalent hydrogen (WEH %) The *Fig*. 2 Average Temperature map was produced directly from Diviner observations [9]. Average illumination maps were derived from a model of south polar illumination as measured on LOLA topography over several lunar precessions [13]. Maps are composed of 5x5 km pixels. Maps are derived from NASA's Planetary Data System archives [14].

Results: *Figure 1* shows the Moon's south polar map of hydrogen above 83°S as derived from LEND's collimated sensor. *purple* areas show the greatest H concentrations associated with the largest PSR's at Cabeus-1, Haworth, Shoemaker, and Faustini (CHSF) craters. The greatest H concentrations and thermal variability occur in the Cabeus-1 PSR. Within the CHSF PSRs, concentrations are biased towards the base of poleward facing slopes, suggesting either downslope migration with accumulation of volatiles at the slope base, thermally constrained loss rates, or the existence of H at shallower depths.

LEND CSETN's high spatial resolution is illustrated in 1) the detection of more anhydrous, partially illuminated crater ridges, 15-20 km width *green*, between the Haworth, Shoemaker, and Faustini PSR's, *blue.* (2) A transect of Cabeus PSR, through the Lunar CRater Observation and Sensing Satellite (LCROSS) impact point (not shown), shows the full-width spatial response of CSETN at 37 km, and provides an *upper-bounds* estimate CSETN's spatial resolution to be 14 km FWHM, consistent with 10 km FWHM published pre-launch [10].

Figure 2 shows the corresponding maximum bolometric maximum surface temperature map derived by Diviner [K]. PSR regions are dark, < 100 K with crater names for the high area PSR class 4) below.

Figure 3 indicates an upper-bounds maximum temperature to entrain H concentration near 110 K. Four classes of decreasing average surface illumination, correlating the class relationships to avg. temperature 1) Illum > 10% 2) 0% < Illum < 10% 3) Low-Area PSR < 125 km^2 4) High-Area PSR > 125 km^2. Low and high area PSR are independently classed by area to reflect their detectability by LEND CSETN. No slope linear fits show no H correlation for the two illuminated classes, 1-2. H correlation to maximum temperature increases for the two PSR classes.

Figure 4 shows the High-Area PSR class 4) pixel distribution as broken down by crater name. The distribution and fit shows a bulk correlation, but the maximum temperature is not a consistent predictor of the H concentrations in the PSRs. However, in the presentation we show that the greatest concentrations, 0.55 WEH % in CHSF are internally consistent with the coldest surfaces. It is not clear why Cabeus has enhanced concentrations of H, yet de Gerlache, Sverdrup, and Slater PSR's, of higher latitude, with similar area and temperature do not.

Figure 1) WEH % with PSR Outlines, 83-90° S

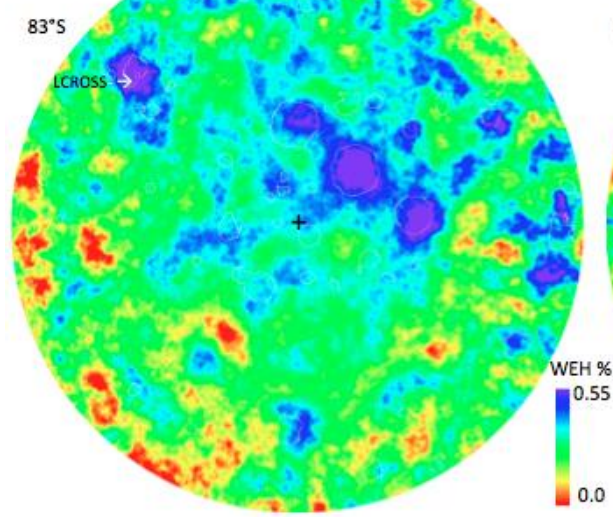

LEND CSETN

Figure 2) Average Temperature, 83-90° S

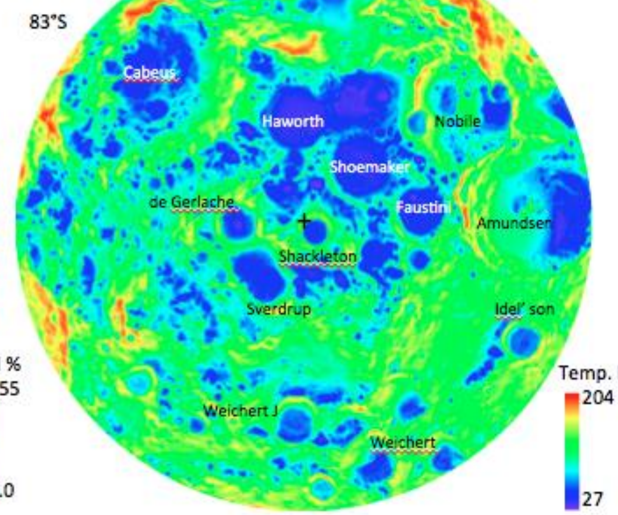

Diviner

Max. Temperature vs WEH % for Four Illumination Classes

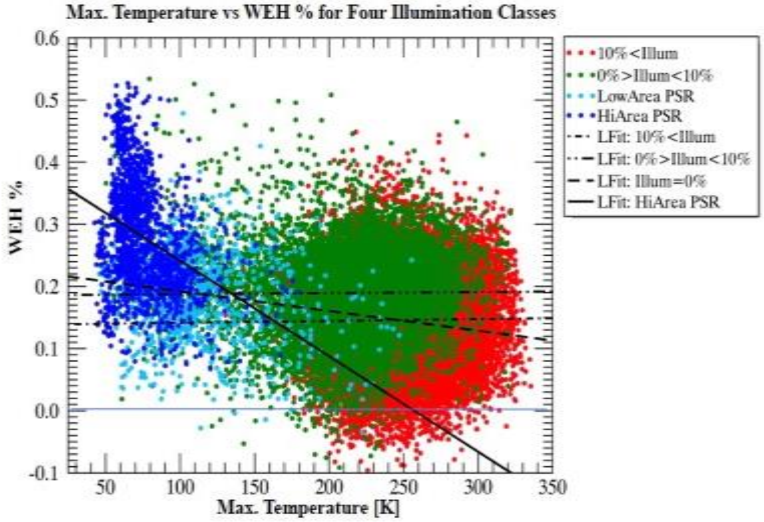

Max. Temperature vs WEH % for the 16 Largest Southern PSR's

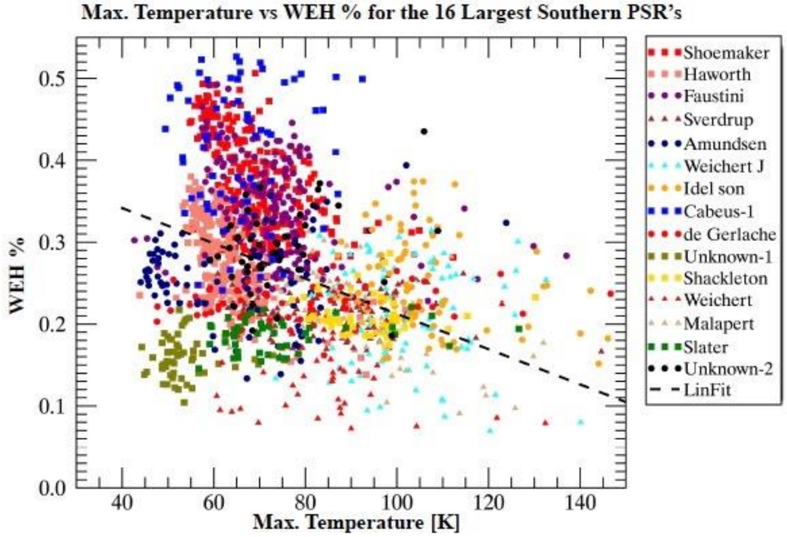

Warmer PSR's, > 55 K, are consistent with diminishing H concentrations towards higher temperatures. Importantly, several PSRs show no significantly enhanced concentrations of H over background.

Conclusions: The illumination and temperature dependent breakdown of the Moon's south polar H map shows an inverse and non-linear bulk relationship towards greater H driven by some PSR's. However, maximum temperature appears is not a consistent predictor of H concentration for many large PSRs, > 125 km^2, suggesting H depositional processes may vary. The presentation will also consider topographic, illumination and other factors thought to control H concentrations.

References: [1] Watson *et al., JGR* 66-9 3033-3045 (1961) [2] LEAG Volatiles Spec. Action Team (2014) [3] Colaprete *et al., Science* (330)-6003 463-468 (2010) [4] Mitrofanov *et al, Science* (330)-6003 (2010) [5] Boynton *et al., JGR-Planets* (117)-E12 (2012) [6] Sanin *et al., JGR-Planets.* (117)-E12 (2012) [7] Lucy *et al., LEAG* (2014) [8] Hayne *et al., LEAG* (2014) [9] Chin *et al., Sp. Sci Rev.* (129)-4 (2010) [10] Mitrofanov *et a*l.(2010) *Sp. Sci. Rev., 150(1-4)* [11] Smith et al.(2010) *Sp. Sci. Rev., 150(1-4)* (2010) [12] Paige *et al., Sp. Sci. Rev*. 150(1-4) [13] Mazarico et al., (2011) *Icarus*, (211) 1066-1081 [14] *Planetary Data System [15] Sanin et al., Icarus (2014) [16] Little et al., JGR 108-E5 (2006)*